The Abdus Salam International Centre for Theoretical Physics

United Nations Educational, Scientific and Cultural Organization

IAEA International Atomic Energy Agency

2167-21

Advanced School on Direct and Inverse Problems of Seismology

27 September - 8 October, 2010

Regional Stress Field Determination

F.H. Cornet

Institut du Physique du Globe de Strasbourg
France

Regional Stress Field Determination

F.H. Cornet; Inst. Phys. du Globe de Strasbourg (France);
françois.cornet@eost.u-strasbg.fr

Talk 1 : Basic concepts

1. Some elementary Rock Mechanics principles
2. Seismicity induced by fluid pressure variations
3. Regional stress field determination

Talk 2 : Local heterogeneity and regional trends

1. The Le Mayet de Montagne experiment
2. The Soultz/Forêts experimental geothermal site in the Rhine Graben (France)
3. Stress field near the Philippine Fault, at Leyte Island

Talk 3 Identifying creep in slow deformation zones

1 Stress field in sedimentary formations

2. Identifying creep location in the Corinth Rift

Some Elementary Rock Mechanics principles

- The stress vector and the Mohr circles
- Griffith's fracture criterion and Irwin's basic fracture modes
- The mechanics of hydraulic fracturing
- Stress failure criteria for rock masses in compression
  - Failure criteria for intact rocks
  - Failure along preexisting weakness planes
  - Failure development in the rock mass

Stress tensor and Stress vector

- For the surface S with unit area and normal **n** centered at **x,** the stress vector is defined as a function of the stress tensor σ and of the surface orientation **n** :

$$\mathbf{t} = \sigma(\mathbf{x})\ \mathbf{n} \qquad (1)$$

- The stress vector has a normal component, (called the normal stress, it is a scalar)) :

$$\sigma_n = \sigma(\mathbf{x})\ \mathbf{n}\ .\ \mathbf{n} \qquad (2)$$

- and a shear component (vector):

$$\tau = \sigma(\mathbf{x})\ \mathbf{n} - (\sigma(\mathbf{x})\ \mathbf{n}\ .\ \mathbf{n}\ )\ \mathbf{n} \qquad (3)$$

- The stress tensor has 6 components defined either in a general (geographical) frame of reference (σ_{ij}), or in the frame of reference of its eigen vectors (σ_i ; φ, ψ, θ = Euler angles that define the 3 eigen vectors orientation $\mathbf{e}_i$)

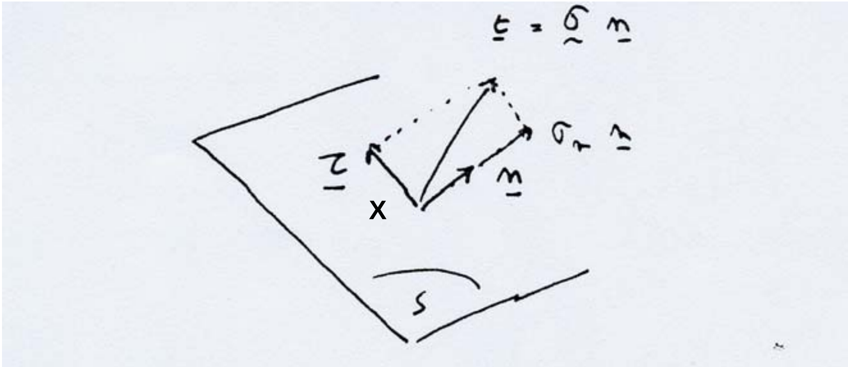

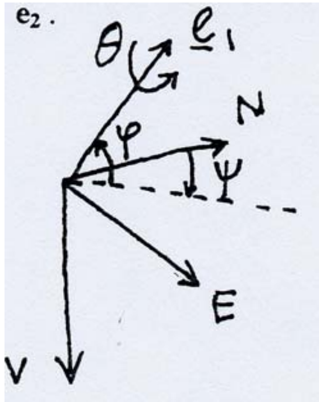

Mohr representation

- Given that σ_n and $|\tau|$ vary with the orientation of **n**, the set of all couples of values σ_n and $|\tau|$ corresponds to the area limited by the three Mohr circles

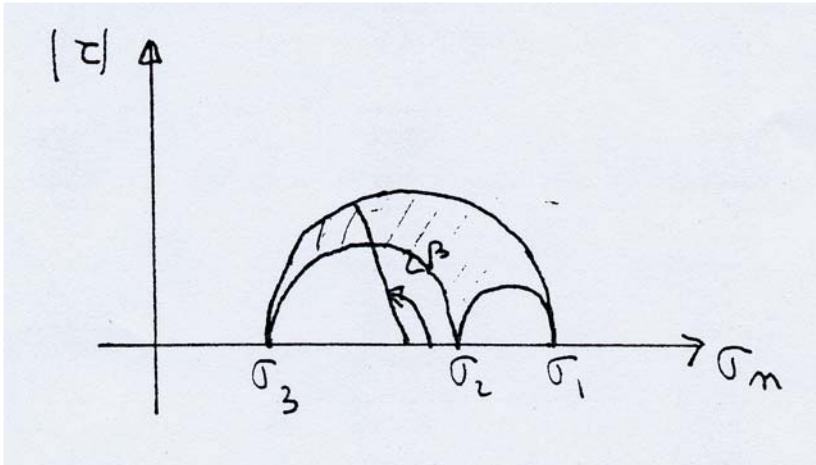

- When n is perpendicular to e_2 , the values for σ_n and $|\tau|$ are :

$$\sigma_n = (\sigma_1 + \sigma_3) / 2 + [(\sigma_1 - \sigma_3)/2] \cos (2 \beta)$$

$$|\tau| = [(\sigma_1 - \sigma_3) / 2] \sin (2 \beta)$$

Where β is angle of **n** w.r. to σ_1 direction

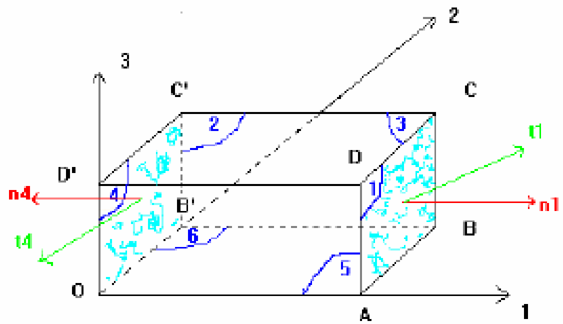

- In rock mechanics, the stress tensor is supposed to be uniform within an Elementary Representative Volume (ERV)

The role of microfissures on the local stress field (from Jaeger, Cook and Zimmermann, fundamentals of rock mechanics, 2007)

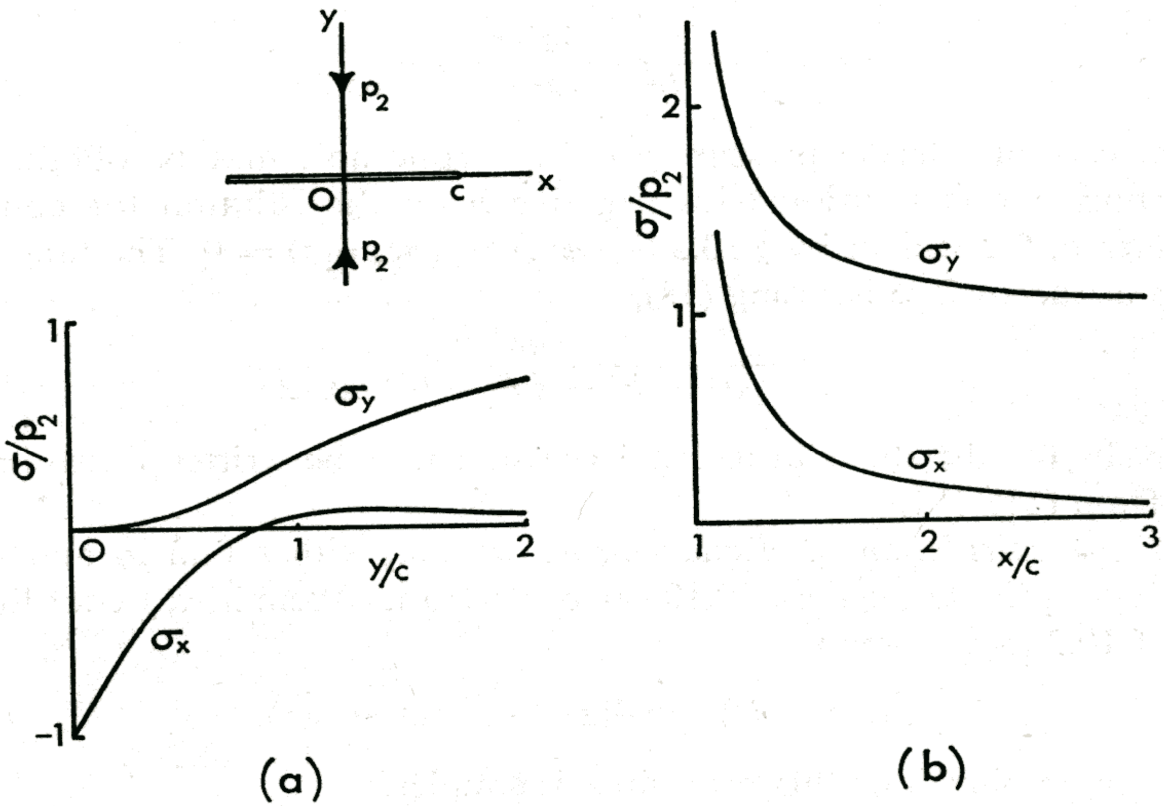

Fig. 10.11.2 Stresses for an elliptic crack of length $2c$ with stress p_2 at infinity perpendicular to its plane. (*a*) Stresses on the *y*-axis. (*b*) Stresses on the *x*-axis.

The Griffith energy criterion of failure

- ΔW (**ds**) = ΔU (**ds**) + ΔT (**ds**) + ΔD (**ds**)
  - Crack increment **ds** = **n**da
  - ΔW (**ds**) : work of external forces
  - ΔU (**ds**) : Elastic strain energy variation
  - ΔT (**ds**) : variation in kinetic energy
  - ΔD (**ds**) : variation in surface energy = γ da, with γ surface energy per unit area

- Strain Energy Release Rate : G = lim (ΔW (**ds**) - ΔU (**ds**)) / da when da $\rightarrow$ 0
- In adiabatic processes, there is rupture when G = 2 γ

  If dG / da < 0 ; fracture growth is stable; if dG / da > 0 ; fracture growth is unstable

- Kaiser effect : seismic signal generated by stable fracturing process; if the load is maintained constant activity stops. When load is increased, the fracturing starts again but does not lead to large scale instability

Irwin’s basic modes of fracture

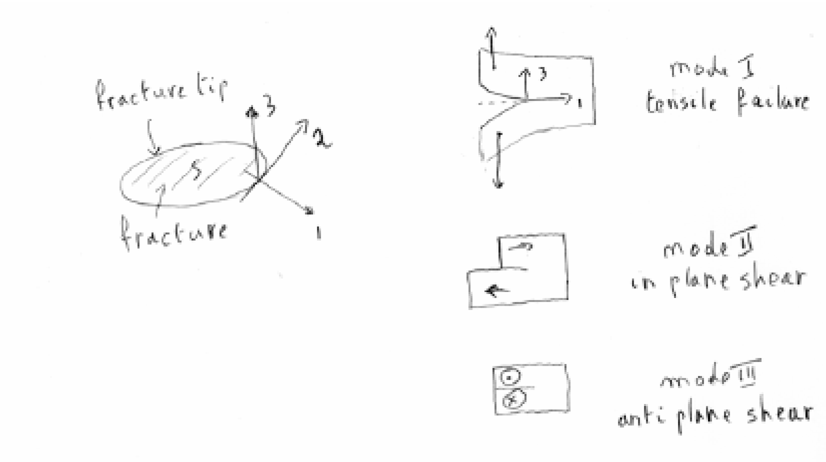

- Because the elastic strain energy variation is entirely dependent on the stress singularity close to the fracture tip, it suffices to investigate values of G close to the fracture tip . Three basic mode of fracture are defined
- Each basic mode is characterized by the stress intensity factor that characterizes the stress singularity near the fracture tip. It is an elastic problem (K_I, K_{II}, K_{III}).
- The stress intensity factors help compute the elastic strain energy released by fracture propagation, a quantity that is equated with the surface energy through the critical strain energy release rate.

Hydraulic fracturing

- The stress field close to a cylindrical hole in an elastic field is :

$$\sigma_{\rho\rho} = \left[1-\frac{r^2}{\rho^2}\right]\frac{\sigma_{11}^{\infty}+\sigma_{22}^{\infty}}{2} + \left[1-\frac{4r^2}{\rho^2}+\frac{3r^4}{\rho^4}\right]\left[\frac{\sigma_{11}^{\infty}-\sigma_{22}^{\infty}}{2}\cos 2\theta + \sigma_{12}^{\infty}\sin 2\theta\right]$$

$$\sigma_{\theta\theta} = \left[1+\frac{r^2}{\rho^2}\right]\frac{\sigma_{11}^{\infty}+\sigma_{22}^{\infty}}{2} - \left[1+\frac{3r^2}{\rho^2}\right]\left[\frac{\sigma_{11}^{\infty}-\sigma_{22}^{\infty}}{2}\cos 2\theta + \sigma_{12}^{\infty}\sin 2\theta\right]$$

$$\sigma_{zz} = \sigma_{33}^{\infty} - 4\nu\frac{r^2}{\rho^2}\left[\frac{\sigma_{11}^{\infty}-\sigma_{22}^{\infty}}{2}\cos 2\theta + \sigma_{12}^{\infty}\sin 2\theta\right]$$

$$\sigma_{\theta z} = \left[1+\frac{r^2}{\rho^2}\right](\sigma_{23}^{\infty}\cos\theta - \sigma_{31}^{\infty}\sin\theta)\,;\quad \sigma_{z\rho} = \left[1-\frac{r^2}{\rho^2}\right](\sigma_{31}^{\infty}\cos\theta + \sigma_{23}^{\infty}\sin\theta)$$

$$\sigma_{\theta\rho} = \left[1+\frac{2r^2}{\rho^2}-\frac{3r^4}{\rho^4}\right]\left[\frac{\sigma_{22}^{\infty}-\sigma_{11}^{\infty}}{2}\sin 2\theta + \sigma_{12}^{\infty}\cos 2\theta\right]$$

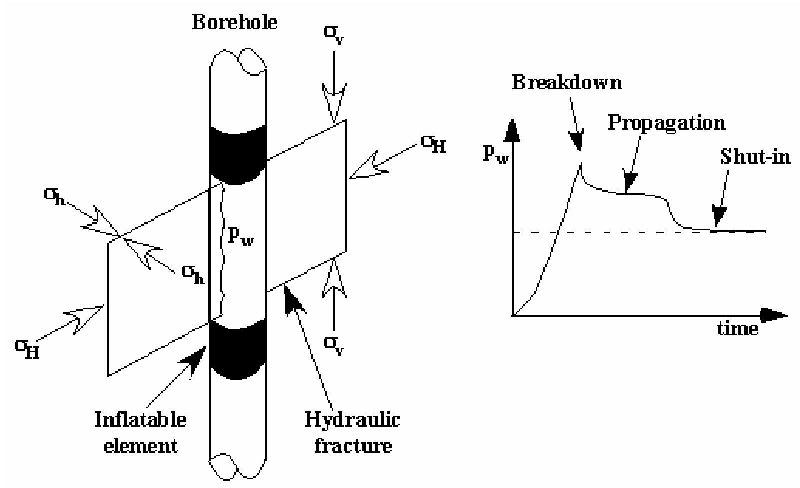

- If the borehole is parallel to a principal stress direction (Vertical) and a pressure is applied in the hole: $\sigma_{\theta\theta} = (\sigma_H + \sigma_h) - 2(\sigma_H - \sigma_h)\cos 2\theta - P_w$, and rupture occurs for :

$$\sigma_{\theta\theta} = -\sigma_H + 3\sigma_h - P_w + \sigma^T$$

- If the rock has been cooled down by mud circulation, the hoop stress is : $\sigma_{\theta\theta} = -K\Delta T/E$, where K is coefficient of thermal expansion, E is Young's modulus and ΔT is the difference between far-field and borehole temperature

Stress criteria for failure in compression

- Intact rocks
  - Tresca criterion

    $$(\sigma_1 - \sigma_3) = K$$
  - Coulomb criterion (fracture orientation depends on stress field)

    $$|\tau| = \mu \, \sigma_n + C_0$$
  - Mohr Envelope
  - Effective stress principle

    $$\sigma' = \sigma - P\,\mathbf{I}$$
- Failure along pre-existing weakness planes
  - Coulomb's friction law (failure plane is imposed) :

    $$|\tau| = \mu \, (\sigma_n - P) + C_0$$
  - Byerlee's law

    $$|\tau| = \mu \, (\sigma_n - P); \; 0.6 \leq \mu \leq 0.8$$

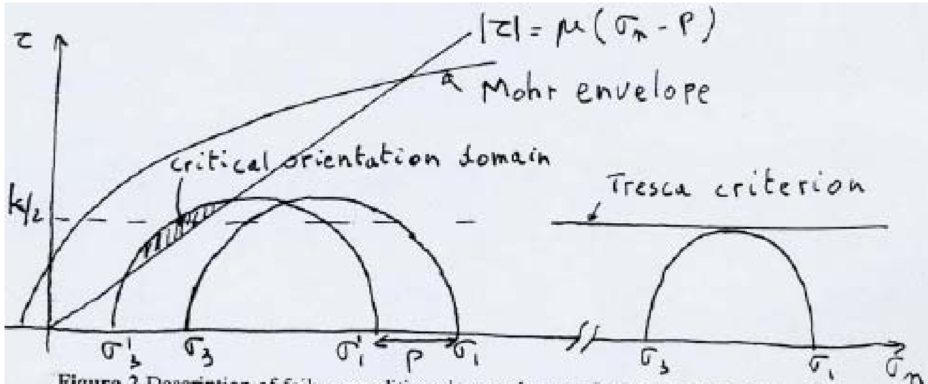

Figure 2 Description of failure conditions in a rock mass. It includes both, failure in the intact rock and failure along preexisting weakness planes as expressed in terms of effective stresses.

- Seismicity occurring in the upper 15 to 20 km of the crust involves fracture planes that make an unknown angle with respect to the principal stress directions.
- Shear displacement along preexisting fractures (faults ?) results in dilatancy and then contractancy

Acoustic emission during triaxial testing and the Kaiser effect

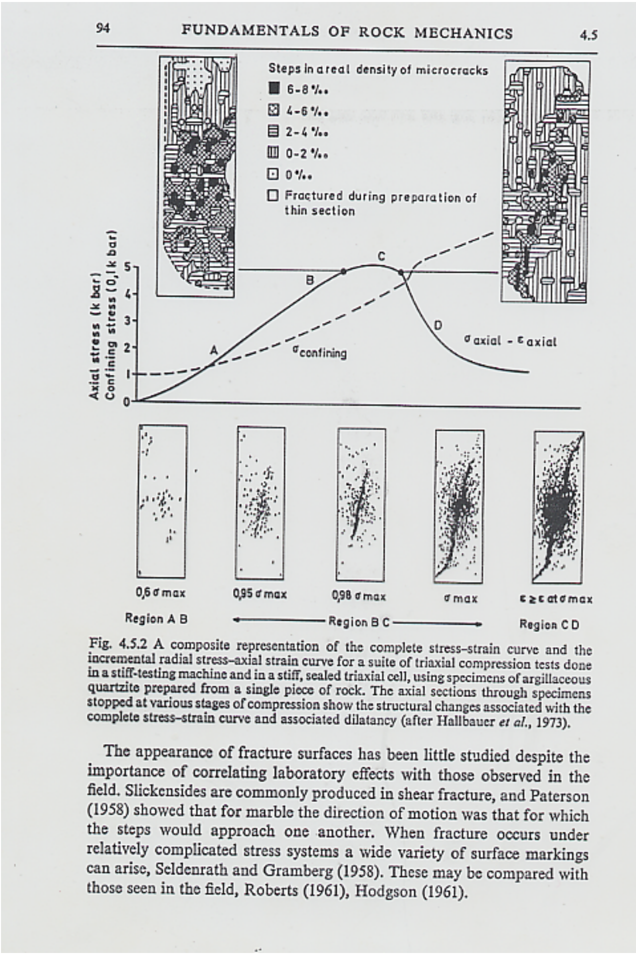
94 FUNDAMENTALS OF ROCK MECHANICS 4.5

Fig. 4.5.2 A composite representation of the complete stress–strain curve and the incremental radial stress–axial strain curve for a suite of triaxial compression tests done in a stiff-testing machine and in a stiff, sealed triaxial cell, using specimens of argillaceous quartzite prepared from a single piece of rock. The axial sections through specimens stopped at various stages of compression show the structural changes associated with the complete stress–strain curve and associated dilatancy (after Hallbauer *et al.*, 1973).

The appearance of fracture surfaces has been little studied despite the importance of correlating laboratory effects with those observed in the field. Slickensides are commonly produced in shear fracture, and Paterson (1958) showed that for marble the direction of motion was that for which the steps would approach one another. When fracture occurs under relatively complicated stress systems a wide variety of surface markings can arise, Seldenrath and Gramberg (1958). These may be compared with those seen in the field, Roberts (1961), Hodgson (1961).

- In the elastic domain, acoustic emission occurs only when the axial load is raised above the largest value that has been reached in previous loading history.
- Question : How long does the rock keeps a memory of its past loading history ?
- How is the onset of macroscopic fracture growth defined ?

On the sources of seismic activity generated by fluid pressure variations

Sileny J, L. Eisner, D.P. Hill and F.H. Cornet; 2009 Non double couple mechanisms of microearthquakes induced by hydraulic fracturing; Jou. Geophys. Res., vol. 114, B08307, doi:10.1029/2008JB005987

- $(\sigma_3 - P_0) > 0$ and Max $[(\sigma_1 - P_0)-(\sigma_3 - P_0)]$ < Elastic limit : Increase in the maximum effective differential stress : Kaiser effect; has been used as a mean to estimate the rock mass hydraulic transmisivity (Shapiro et al., 1997)

- $(\sigma_3 - P_0) > 0$ and Max $[(\sigma_1 - P_0)-(\sigma_3 - P_0)]$ > Elastic limit (Modes II and III), or effective Coulomb stress ($[\tau - \mu(\sigma_n - P_0)]$ larger than fault cohesion C_0, failure in shear, eiher through a fresh plane but most often on a preexisting fault

  These are shear fractures that should generate double couple with their nodal planes inclined w.r. to fracture plane, because double couple only represents dynamic elastic response to shear stress drop during rupture.

- $(\sigma_3 - P_0) < 0$:Hydraulic fracture propagation in mode I
  - Uniform pressure P up to fracture tip :
    $K_I \propto (\sigma_{min} - P)\sqrt{\pi a}$; fracture is unstable
  - No fluid penetration, pressure P in borehole :
    $K_I \propto (\sigma_{min} - P)\, 1/\sqrt{a}$; fracture is stable

  These are tensile cracks and should generate dipoles with main axis more or less perpendicular to fracture plane; the unstable crack length is in smaller than 1 m, hence signals are very high frequency (> 100Hz)
  - The Hill mesh scheme

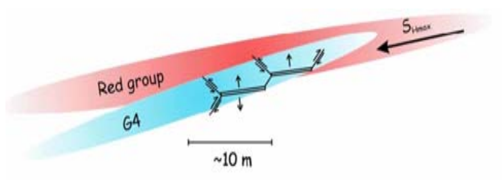

- Stress redistribution because of large scale pressure variation within the reservoir, or within the stimulated zone (also observed when pore pressure decreases).

- Resonances : long period events; tremors, trapped waves

Monitoring Seismic activity generated by fluid pressure variations

- While shear events (quadrupoles) are often in the 10 – 500 Hz range, dipoles from the crack tip are much shorter and require high frequency sensors, close to the fracture tip;

- Monitoring hydraulic fractures requires downhole instrumentation and a few companies have specialized in this operation.

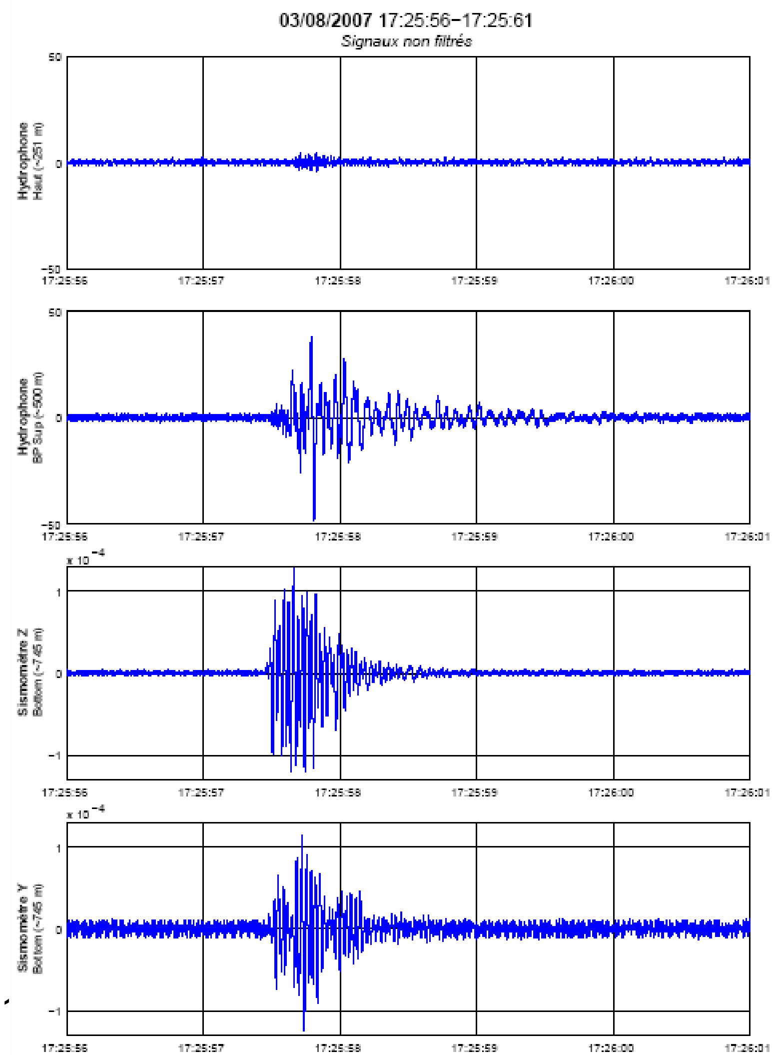

Determination of the regional stress field

Main techniques :

- From cores, because rocks are visco-elastic and keep some memory of past loads;
- From underground cavities (flat jacks, overcoring)
- From boreholes (overcoring, hydraulic testing, boreholes wall failure analysis)
- From focal mechanisms
- From seismic anisotropy

Stress determination from Hydraulic Fracturing

(for more details, Haimson B.C. and F.H. Cornet; 2003 ISRM Suggested Methods for rock stress estimation; Part III:Hydraulic fracturing methods ; Int. Jou. Rock. Mech. Min. Sc., vol. 40, 7/8, pp 1011-1020

- Hydraulic Fracturing
  - Valid only if borehole is parallel to a principal stress direction.
  - Frac orientation yields maximum Horizontal principal stress direction
  - Shut in pressure (stabilization of pressure when injection stops) yields minimum horizontal principal stress magnitude
  - Breakdown pressure yields maximum Horizontal principal stress magnitude
  - But problem for taking into account pore pressure in breakdown equation and difficulty for determining “tensile strength”

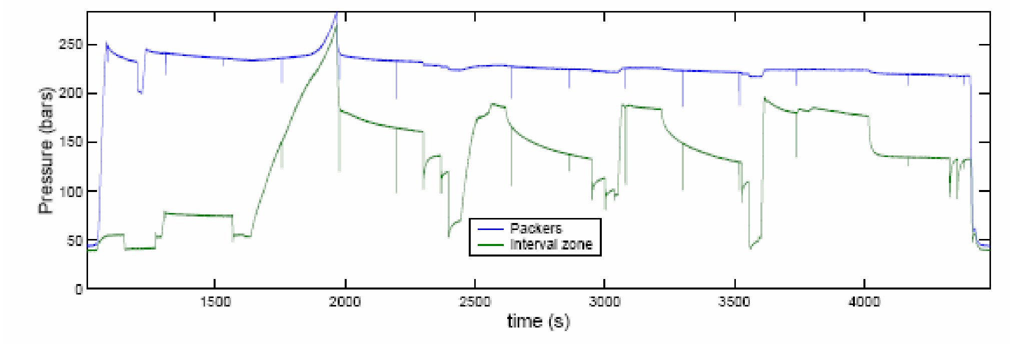

$$\sigma_{\theta\theta} = - \sigma_H + 3\ \sigma_h - P_w + \sigma^T$$

Ultrasonic Borehole imaging of Hydraulic fracture

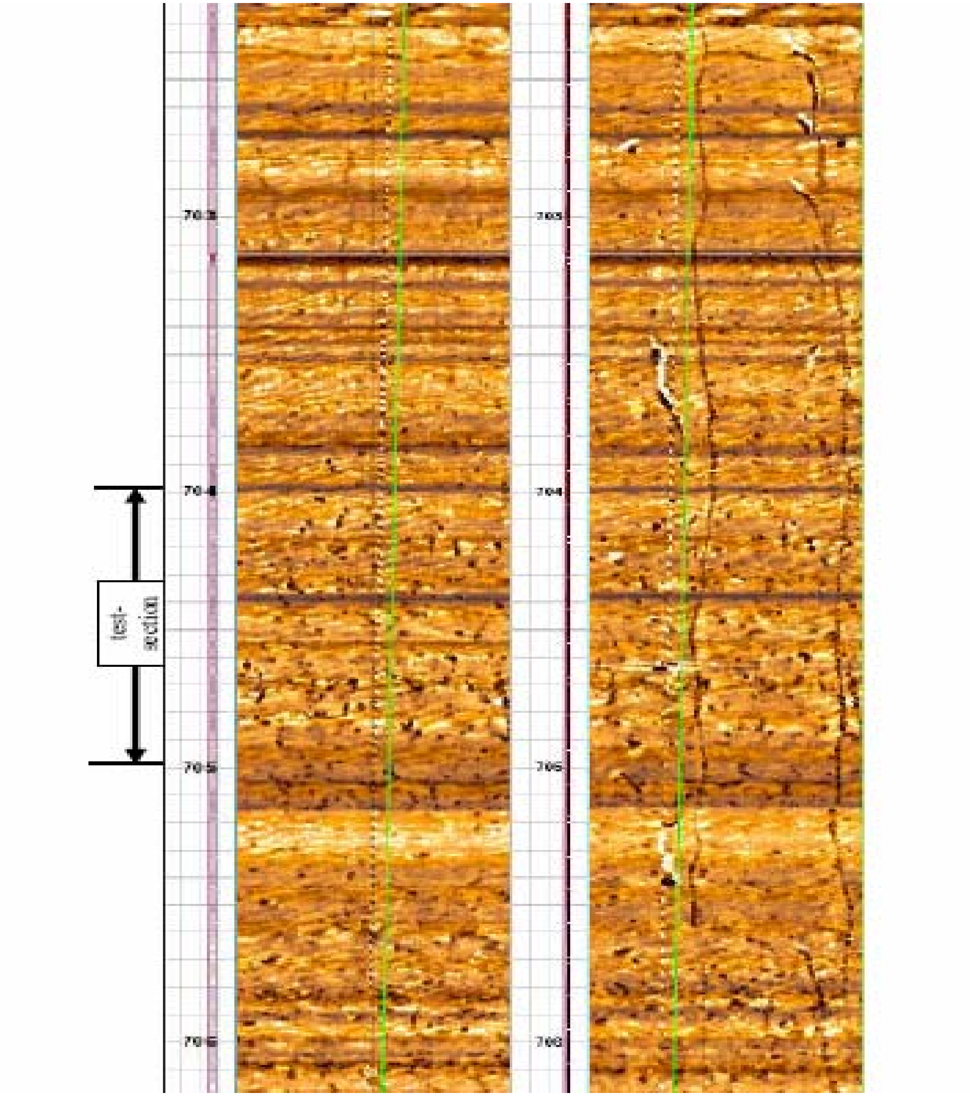

Ultrasonic Borehole Image (UBI) of a hydraulic fracture. On the left before testing (no fracture seen), on the right after hydraulic testing : the logging shows the vertical fracture that extends, in this case, beyond the packed off interval.

Imaging logs (electrical or ultrasonic), provide much longer borehole coverage than traditional impression packers and help determine whether the fracture remained constrained in the packed off interval

Stress determination from Reopening preexisting fractures (HTPF)

- Preliminary electrical imaging log yields images of « preexisting » fractures

- Hydraulic testing on preexisting fracture yields normal stress supported by corresponding fracture : $\sigma_n = \sigma \mathbf{n} . \mathbf{n}$

- If more than 6 different directions are tested, then the 6 components of σ may be determined

- In practice integrate HF and HTPF : 3 to 4 HF tests yield direction and magnitude of minimum principal stress while 2 to 3 HTPF tests yield magnitude of other principal stress components

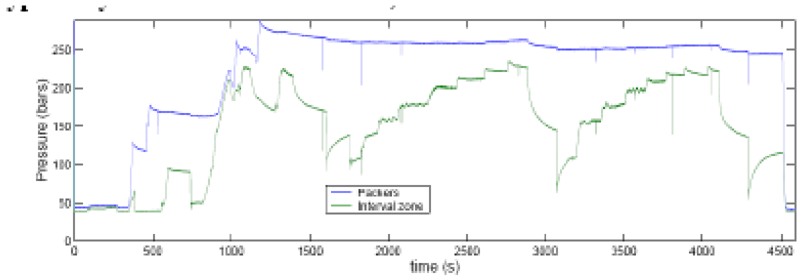

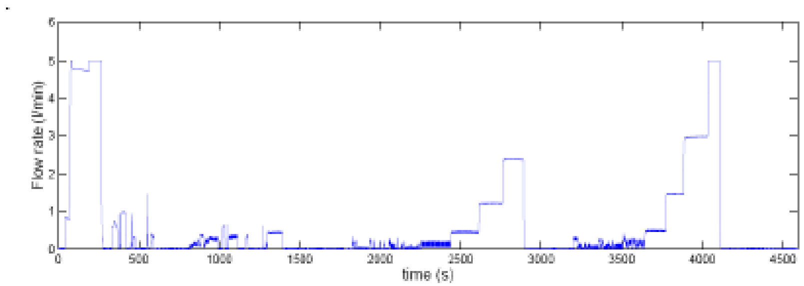

- But problem with quasistatic reopening tests if fracture is inclined to borehole direction; Hence better use only shut-in pressure tests

$$\sigma(x_3) = \sigma(x_c) + (x_3 - x_{3c})\,\alpha$$

Stress determination from borehole failure analysis

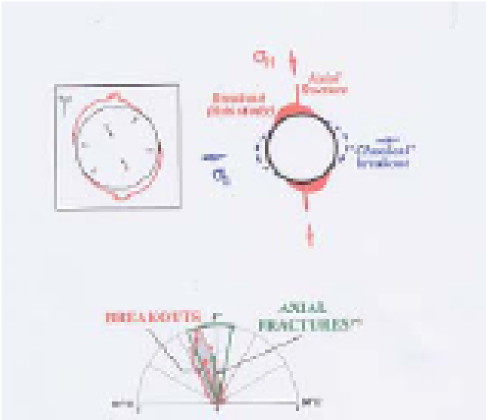

- Tangential stress at the borehole wall

  $\sigma_{\theta\theta} = (\sigma_h + \sigma_H) - 2(\sigma_H - \sigma_h)\cos 2\theta - P_b - f(P_o) - \alpha E\Delta\theta / (1-\nu) - 3/8\ \Delta\alpha E/(1-\nu)\ \Delta\theta$

  Where $\Delta\alpha$ is the mismatch between thermal expansion coefficients (solution for square inclusion in an homogeneous matrix)

- Time dependency of cooling :
  - Slow cooling yields borehole elongation (thermal breakouts),
  - fast cooling yields macroscopic thermal cracking

Breakouts and tensile induced fractures are well detected with borehole imaging tools such as the Ultrasonic borehole imager or the Electrical Formation Imager.

Ultrasonic imaging (UBI)

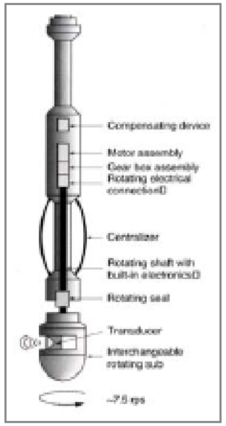

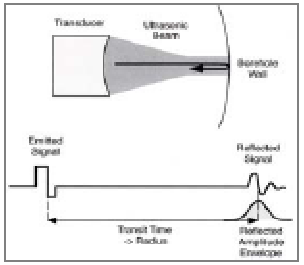

Information from double couple focal mechanisms

- **Data produced by fault plane solutions**

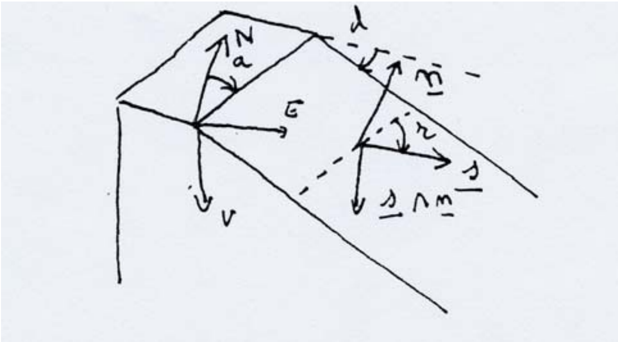

- Focal mechanisms of pure shear faults (no significant dilatancy), yield for both nodal planes the dip and azimuth of the plane (d and a) as well as the slip direction in the plane (rake angle r of slip vector **s**) when it corresponds to the fault plane
- (a1, d1, r1, εa1, εd1, εr1 , a2, d2, r2, εa2, εd2 , εr2).

- **Principle of inversion** : **s** . τ ***/*** **|**τ**|** = 1

τ Resolved shear stress in plane

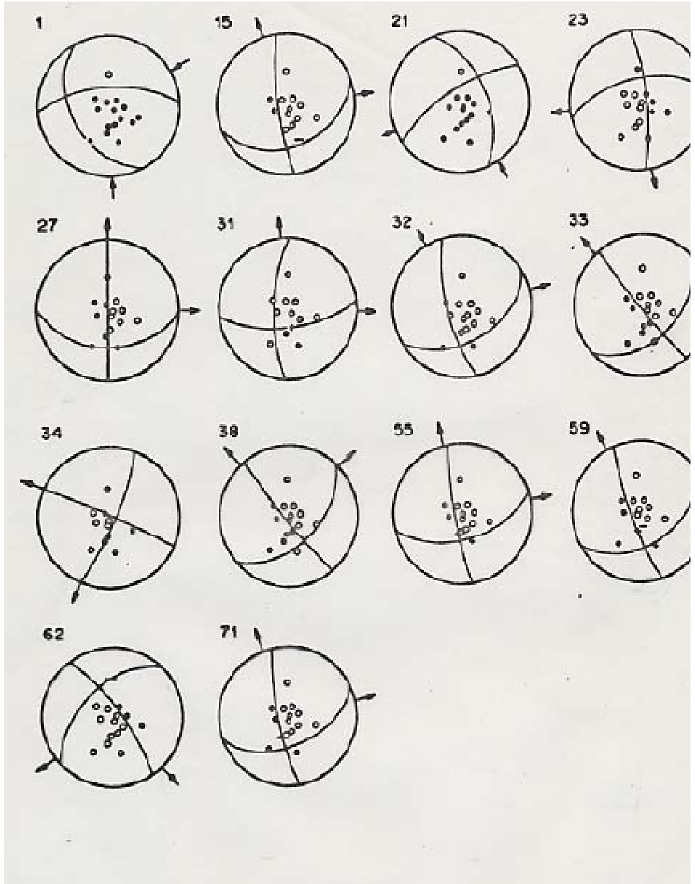

Focal mechanisms of induced seismicity during the initial reservoir development

Gephart & Fosyth's approximate method – 1

Gephart and Forsyth, Jou. Geophys. Res., 1984

- Basic assumptions
  - Slip occurs parallel to the direction of the resolved shear stress.
  - All seismic events are distant enough from each other so that the stress perturbation induced by each event does not alter the stress field for other events.
  - The original stress field is uniform within the volume sampled by the various events
- The stress is decomposed as :
  $\sigma = \sigma 1\ \mathbf{I} + (\sigma 3 - \sigma 1)\ \mathbf{T}$

In which T has the same principal directions as σ and O, R and 1 as eigen values, with

$$R = (\sigma 2 - \sigma 1) / (\sigma 3 - \sigma 1)$$

- We consider two frame of reference, Q corresponds to the eigen vectors of **T,** and Q' is associated with the fault plane (normal **n**, slip vector **s** and **n^s**).

- For tensor T to be compatible with a given slip vector in a given fault plane, it is necessary that :

$$R = - \beta_{13} \beta_{23} / \beta_{12} \beta_{22}$$

Where β_{ij} are the components of the orthogonal tensor that rotates Q to Q'

The idea is to explore the set of all possible solutions and to identify that which fits best observations, namely the tensor that yields resolved shear stress directions closest to observed slip vector directions.

But uncertainties exist on all angles.

The problem is three folds :

- Identify for each focal mechanism which nodal plane is the fault plane;
- For all focal mechanisms define a measure of their misfit with a given tensor **T.**
- Identify the best solution and associated confidence level domains.

Gephart & Fosyth's approximate method - 2

- Identification of fault planes and measure of misfit
  - For any given nodal plane, identify smallest rotation of plane required to bring **s** parallel to τ
  - For a given tensor **T,** chose as fault plane, for each focal mechanism, that which requires the smallest rotation.
  - Characterize the misfit, for the corresponding tensor **T,** by the quantity (L1 norm) :

$$m_l = \sum_{k=1}^{N} \min(x_k^l, l = 1,6)$$

X_k^l is the l^{th} rotation for focal plane solution k.

- Identification of solution : given $0 \leq R \leq 1$, and given Euler angles range from 0 to 360°, the complete domain of possible solutions is explored. The solution is that which yields the smallest misfit.

- 64% and 90% confidence level with L1 norm complete the characterization of the solution

Table 1

Expressions for rotations about axes of fault plane geometry.

Rotation axis	Algorithm	Period
n	$\theta = -\tan^{-1}\left[\frac{RB_{12}B_{22} + B_{13}B_{23}}{RB_{12}B_{32} + B_{13}B_{33}}\right]$	Π
s ∧ **n**	$\theta = \tan^{-1}\left[\frac{RB_{12}B_{22} + B_{23}B_{13}}{RB_{22}B_{32} + B_{23}B_{33}}\right]$	Π
s	$\theta = \frac{1}{2}\tan^{-1}\left(\frac{2}{k}\right)$ where $k = \frac{R(B_{12}^2 - B_{22}^2) + B_{13}^2 - B_{23}^2}{RB_{12}B_{22} + B_{13}B_{23}}$	$\frac{\Pi}{2}$

- The problem with a large ERV

$$\sigma(x_3) = \sigma(x_c) + (x_3 - x_{3c})\,\alpha$$

$$R = (\alpha_2 - \alpha_1) / (\alpha_3 - \alpha_1)$$

Principal stress directions and shear wave splitting

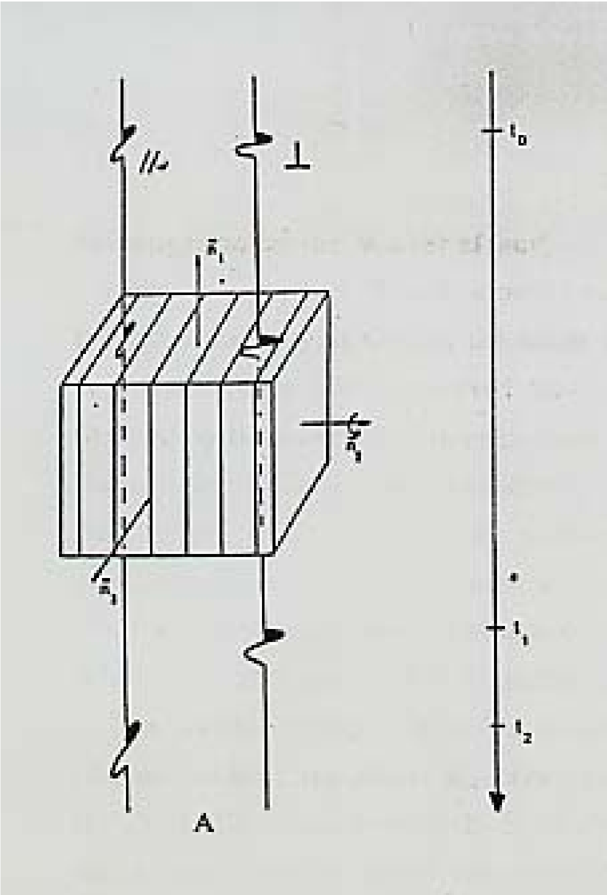

- When rock mass is anisotropic, two shear waves arrivals are detected; their polarization occurs in two perpendicular directions.
- When rocks support a non hydrostatic stress field, the maximum principal stress direction corresponds to a larger Young's modulus than the direction of the minimum principal stress. This results in shear wave splitting, the fastest arrival being in coincidence with maximum principal stress direction.